Tracking Performance Analysis and Simulation of the Digital Pointing System for the Optical Communication Demonstrator

C. Racho[1] and A. Portillo[1]

Over the past 3 years, JPL has been heavily engaged in designing and developing a reduced-complexity optical communication terminal for high-data-volume applications. The terminal is called the Optical Communication Demonstrator (OCD) and has the ability to point microradian-level beams with a very small number of detectors and steering elements. Using only a single steering mirror and a charge-coupled device (CCD) detector array, the OCD can accomplish the functions of beacon signal acquisition, beacon tracking, transmit and receive beam coalignment, and transmit beam point-ahead offset.

At a higher system level, developing an understanding of the OCD performance is an essential part of achieving a better understanding of the end-to-end optical communication system performance in the field. During the latter half of fiscal year 1998, a series of experiments was conducted between Table Mountain and Strawberry Peak using the OCD as a transmitting terminal for terrestrial ground-to-ground optical link demonstrations. The OCD was taken to Strawberry Peak and set up to receive the multibeam laser beacon from the 0.6-meter telescope located at Table Mountain, a distance of approximately 40 kilometers. In the presence of atmospheric effects, the laser beacon will fluctuate both in intensity and position. The ability to determine the performance of the control loop under atmospheric-induced fades and distortion becomes very important in evaluating the results of the field testing.

This article describes the design and performance of the OCD digital control loop system, which includes the steering mirror, the CCD detector array tracker, and the associated electronics. The digital control loop performance is a key factor in the ultimate performance of the laser beacon acquisition and tracking algorithm of the OCD.

A model of the OCD digital control loop is developed for use in simulations. The analytical results from control loop simulations are compared with measured data. The analytical model of an improved steering mirror is substituted into the simulation. The results of the simulation indicate that, in order to realize the benefits of upgrading to a faster steering mirror, the system time delays must be minimized.

[1] Communications Systems and Research Section.

I. Introduction

An important part of the laser communication experiment is the ability of the FSM to track the laser beacon within the required tolerances. The pointing must be maintained to an accuracy that is much smaller than the transmit signal beam width. For an Earth orbit distance, the system must be able to track the receiving station to within a few microradians. The failure to do so will result in severely degraded system performance. This is especially true for the ground-to-ground system that is used in the initial phase of the OCD field experiment.

The goals of this effort were to characterize the end-to-end system performance of the digital controller for the Optical Communication Demonstrator (OCD) and to prepare for the upgrade of the Fast Steering Mirror (FSM) that could substantially improve the tracking performance. To evaluate the tracking performance, the existing system software was modified to collect data that could characterize the FSM, the FSM electronics, and the camera imaging subsystem. The system was measured in both open-loop and closed-loop operating modes. A linear time invariant open-loop model was developed and used in the design of a compensating digital filter. The closed-loop performance was predicted using MATLAB. With the digital filter programmed into the OCD control software, data were collected to verify the predictions. This article presents the results of the system modeling and performance analysis.

II. Laboratory Measurements

A. System Architecture

The OCD design is described in detail in [3,4]. A block diagram of the OCD is shown in Fig. 1 [7]. The OCD forward loop consists of the Texas Instruments TMS320C44 digital signal processor (DSP), which runs the control and imaging software; the digital-to-analog converter (DAC), which converts the digital filter output signal to an analog input signal for the FSM servo interface; the two-axis FSM servo; and the mirror. The FSM position is sensed by way of the CCD, a DALSA CA-D1 camera with a 128-by-128 pixel array modified for windowed readout, which reports a centroid value derived from the CCD image. The FSM is a two-axis beam steerer (TABS) manufactured by General Scanning.

For the purposes of analyzing the mirror control system to improve the laser beacon tracking, the system is grouped conceptually into subsystems (see Fig. 2). The DAC, FSM servo, and mirror are treated as the system plant. The CCD is treated as an element that contributes to the system delay only within the target control-loop bandwidth of 100 Hz and is modeled as such. This does not mean, however, that it is the only element in the loop that contributes to the system delay. The DSP and the DSP software together make up the digital filter.

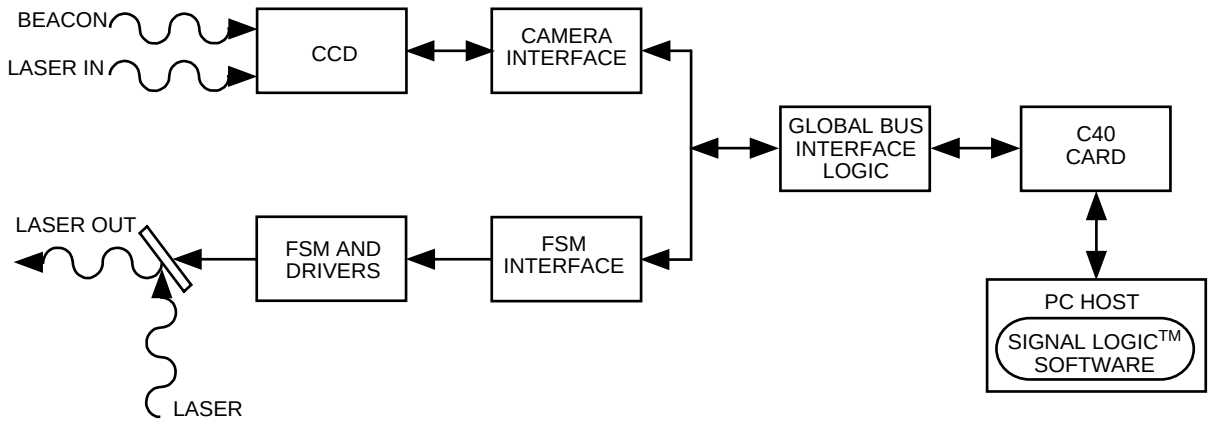

Fig. 1. The OCD system block diagram.

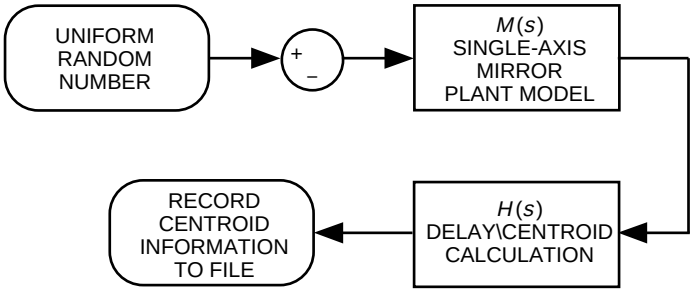

Fig. 2. The OCD mirror open-loop plant modeling block diagram, continuous time.

B. Data Collection

The OCD FSM control law is implemented on a Texas Instruments TMS320C44 DSP. All system code changes, i.e., software written and compiled to run on the DSP, and all data capture are accomplished by way of the Signalogic^{TM} digital signal-processing development environment. The data collected for these experiments were obtained at a real-time system rate of 2 kHz. This system can buffer data sequences up to 4000 points long.

Data gathered for the mirror operating in the open-loop mode were taken by inputing a known signal, such as a sine wave, into the OCD FSM control driver circuitry. The open-loop data were collected for two input cases: a sine wave and a white noise signal. These input digital signals were generated in the DSP software. Each digital input point represents the desired or commanded centroid pixel location, which is essentially how the mirror position is measured. The FSM positions then were determined by reading the CCD-camera-calculated centroid values for the mirror x-axis and y-axis. The values collected for these experiments consisted of the generated input centroid signal and the calculated centroid results from the CCD camera.

In closed-loop operation, the loop is closed around a compensating digital filter. The mirror position, i.e., the centroid calculation, is fed back and subtracted from the desired position. This error then is input to the filter in order to produce the mirror control signal that is applied to the FSM driver control circuit. In the closed-loop mode, a sine wave signal was applied in a way similar to the open-loop method. However, the compensator drives the mirror in an attempt to track the sinusoidal input. The input signal and the feedback centroid information are simultaneously recorded at the sample rate of 2 kHz.

In either the open- or closed-loop mode, the data were obtained for selected discrete input sine wave frequencies. For the open-loop mode, the white noise input was generated by creating a DC signal in which the level was fixed for a given number of sample intervals and was determined by a random-number generator. The update rate for the latter signal was 1 kHz, i.e., the level was fixed for two samples, with a sequence length of 2000 points.

III. Open-Loop Characterization

A model for the open-loop mirror was developed for each axis of the mirror position controller. A white noise signal was injected into the open-loop mirror control system at the input to the loop (see Fig. 2). The digital output and input data were saved to a file and then analyzed in the frequency domain using MATLAB. The procedure used to estimate the frequency response function is described in the Appendix. In addition, digital sine waves at selected discrete frequencies were input to the open-loop system and the data recorded. The magnitude and phase data for both the white noise and sine wave inputs were plotted for each axis. As expected, the two sets of data agree, as shown in Fig. 3.

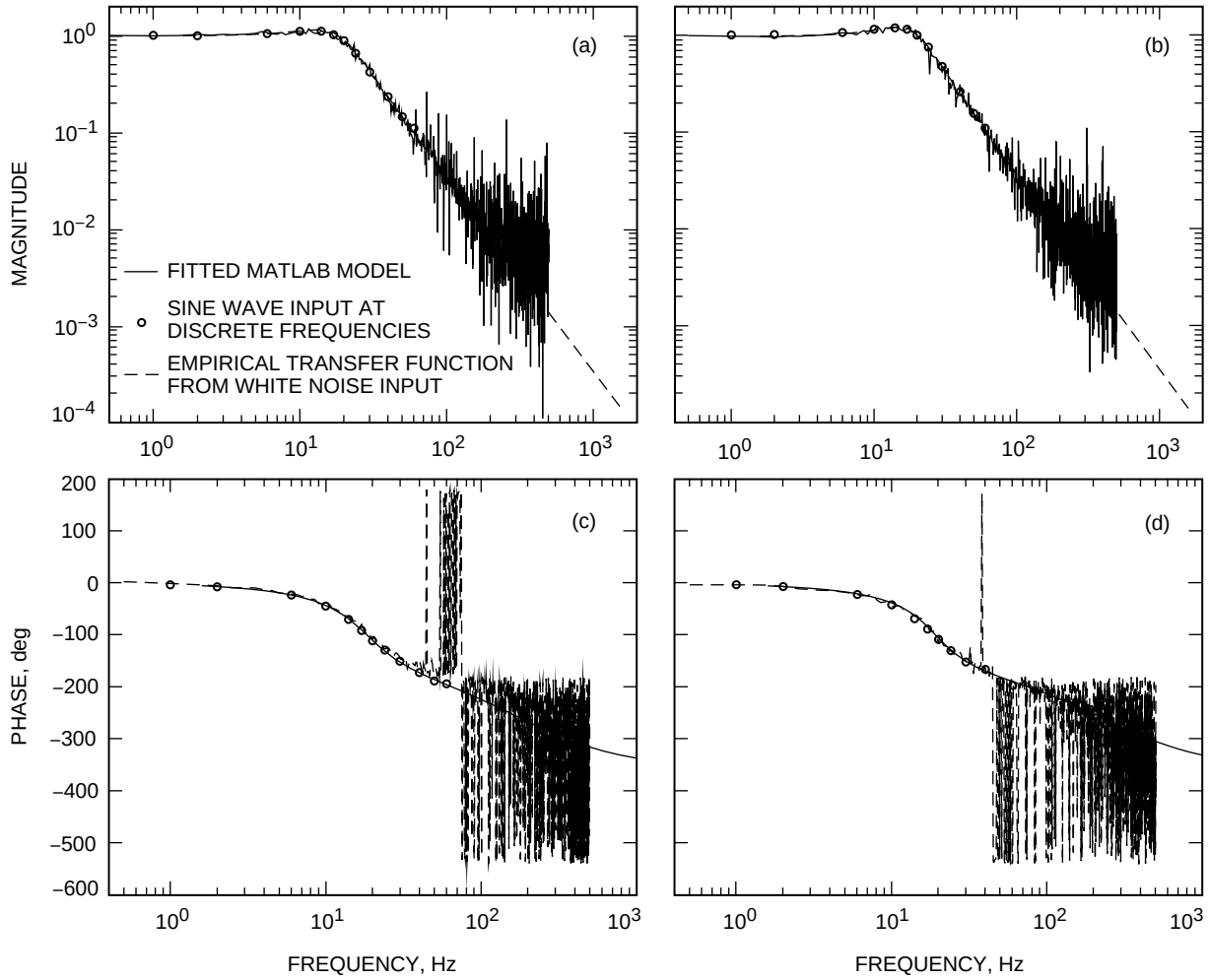

Fig. 3. The OCD mirror open-loop data plots: (a) x-axis magnitude, (b) y-axis magnitude, (c) x-axis phase, and (d) y-axis phase.

A second-order linear time-invariant model was derived empirically using MATLAB by fitting the open-loop data in both amplitude and phase. In Fig. 3, the dashed lines that coincide with the measured responses are the bode plots of the resulting MATLAB models.

The x-axis mirror plant model, $M_x(s)$ in Eq. (1), has a double pole estimated to be at 18.5 Hz with a damping ratio of 0.5; the y-axis mirror plant model, $M_y(s)$ in Eq. (2), has a double pole estimated to be at 19 Hz with a damping ratio of 0.45:

$$M_x(s) = \frac{13,500}{s^2 + 37 \times 2\pi \times 0.5s + (18.5 \times 2\pi)^2} \tag{1}$$

$$M_y(s) = \frac{13,900}{s^2 + 38 \times 2\pi \times 0.45s + (19 \times 2\pi)^2} \tag{2}$$

The additional phase delay attributed to any time delays in the loop, e.g., calculation of the new centroid, is linearly modeled by $H_x(s)$ in Eq. (3) and $H_y(s)$ in Eq. (4):

$$H_x(s) = \frac{-s + \dfrac{2}{T_{dx}}}{s + \dfrac{2}{T_{dx}}} \tag{3}$$

where T_{dx}= 0.00166 second, and

$$H_y(s) = \frac{-s + \dfrac{2}{T_{dy}}}{s + \dfrac{2}{T_{dy}}} \tag{4}$$

where T_{dy}=0.00125 second.

The CCD imaging contributes about 0.5 millisecond to this delay. The remaining time delay most likely is due to the DSP software processing time and the FSM servo, but exactly how much each contributes has not yet been measured.

The resulting modeled open-loop system phase delay can be seen in Figs. 3(c) and 3(d), along with the measured open-loop system phase delay data. (The magnitude responses of the fitted and measured open-loop system are shown in Figs. 3(a) and 3(b).) The fitting parameters, such as gain, phase delay, poles, and damping ratio of the linear model, are varied such that the norm of magnitude and phase of the estimated transfer function minus the fitted transfer is minimized over the frequency range of interest.

IV. Closed-Loop Prediction

Using the MATLAB open-loop plant model, the loop was closed around a continuous time equivalent of the digital filters:[2]

$$C_x(z) = \frac{40[1 - 1.9403z^{-1} + 0.9435z^{-2}]}{1 - 1.1765z^{-1} + 0.1765z^{-2}} \tag{5}$$

$$C_y(z) = \frac{48.39[1 - 1.9435z^{-1} + 0.9465z^{-2}]}{1 - 1.1765z^{-1} + 0.1765z^{-2}} \tag{6}$$

The design is based on pole-zero cancellation or pole shifting where the stable poles of the plant are canceled by zeros of the digital filter and replaced with poles in more desirable locations [1,2]. The conversion of the linear systems from continuous time to discrete time domain and vice versa assumes a sampling frequency of 2 kHz. The closed-loop system for each axis is diagrammed in Figs. 4 and 5. The frequency-domain plots for phase and amplitude of this closed-loop system predicted by the MATLAB models are given in Fig. 6. The x-axis digital filter, $C_x(z)$, was modified slightly to account for the different x-axis plant poles.

[2] The original analytical design work for the digital filters was performed by B. Lurie and S. Sirlin, "Subject: Optical Communication Controller," JPL Interoffice Memorandum to M. Jeganathan (internal document), Jet Propulsion Laboratory, Pasadena, California, January 1997.

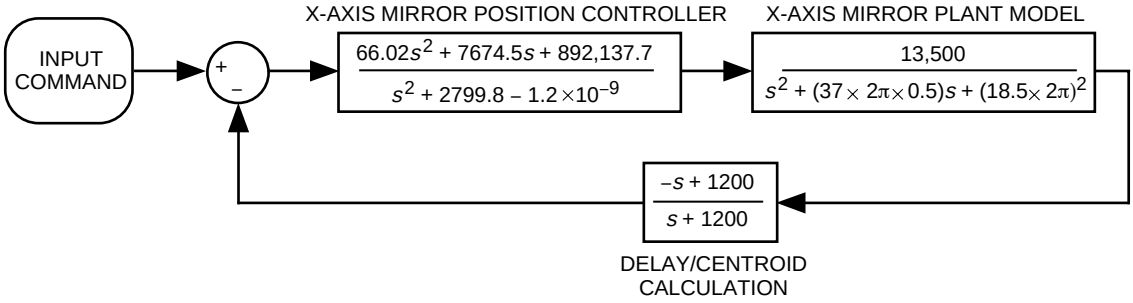

Fig. 4. The OCD x-axis mirror closed-loop control block diagram, continuous time.

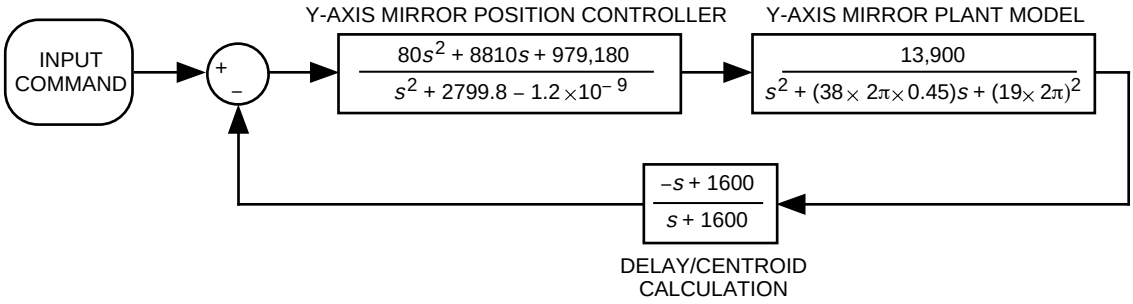

Fig. 5. The OCD y-axis mirror closed-loop control block diagram, continuous time.

The above digital-filter equations were converted to their equivalent continuous time representation in the Laplace domain:

$$C_x(s) = \frac{66.02s^2 + 7674.5s + 892,137.7}{s^2 + 2799.8s - 1.2 \times 10^{-9}} \tag{7}$$

$$C_y(s) = \frac{80s^2 + 8810s + 979,180}{s^2 + 2799.8s - 1.2 \times 10^{-9}} \tag{8}$$

The open-loop transfer function, which includes the compensating filters, is used to determine the gain and phase margins for each axis. The open-loop bode plots for the x-axis transfer function, $C_x(s)G_x(s)H_x(s)$, and the y-axis transfer function, $C_y(s)G_y(s)H_y(s)$, are shown in Fig. 7. The resulting x-axis gain and phase margin are 9.2 dB and 53.73 deg, respectively. Similarly, the y-axis gain and phase margin are 9.4 dB and 53.41 deg, respectively. These margins provide for a measure of the system stability.

V. Closed-Loop Verification

Experimental data were taken to characterize the closed-loop performance with the digital filters in place. The OCD mirror-control system was closed around the digital filters, $C_x(z)$ and $C_y(z)$, shown in Eqs. (5) and (6), which were implemented in the OCD software. The filter gains were adjusted separately for each axis in the math models to achieve approximately 100 Hz of control bandwidth. The closed-loop system then was tested to verify the math model predictions. Sine waves at discrete frequencies and steps were input as position commands into the closed-loop mirror-position control system. Each axis was tested independently. The empirical results are shown along side the predictions in the bode plots in Fig. 6. For the x-axis closed-loop control, the predicted -3 dB bandwidth of the magnitude response was

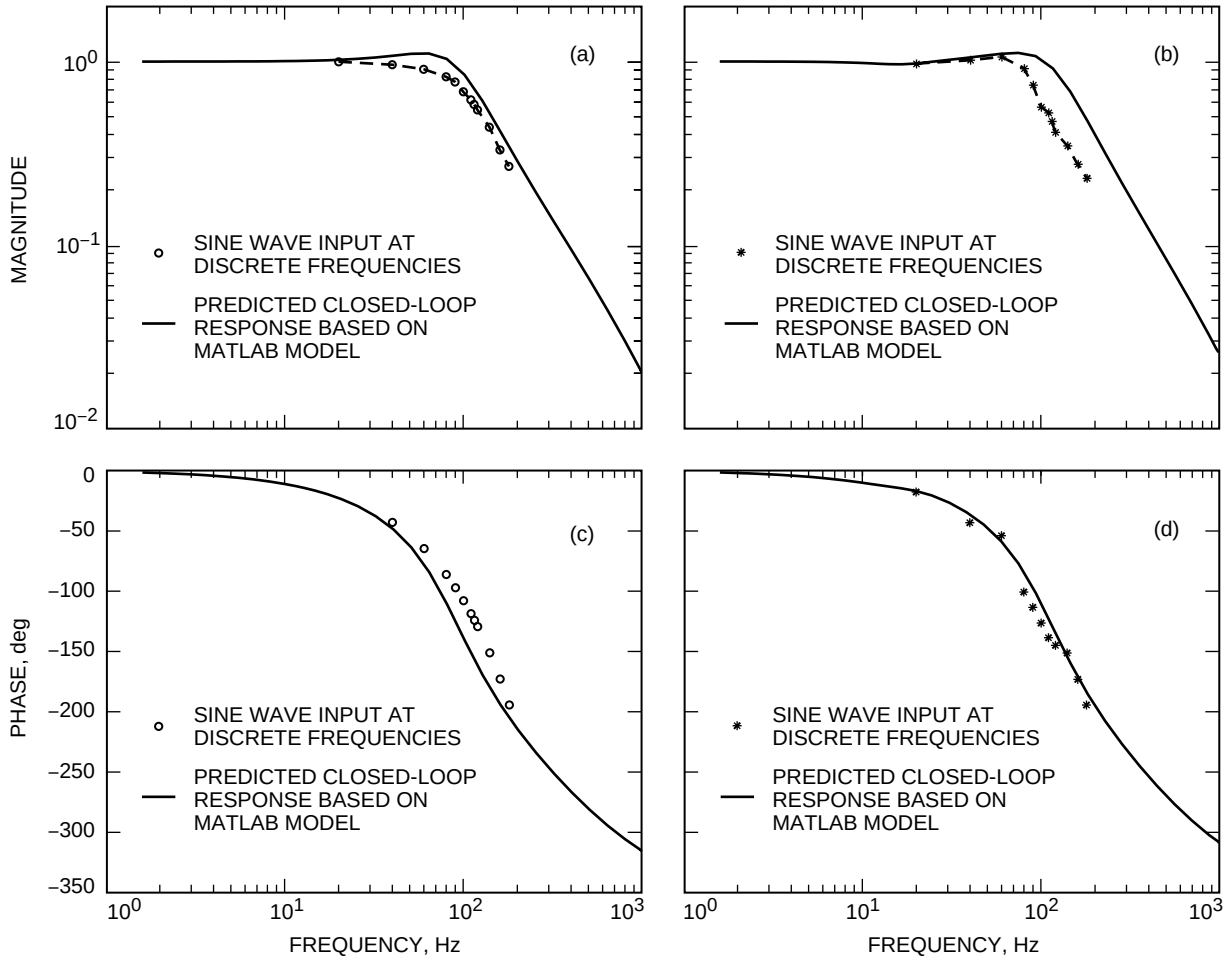

Fig. 6. The OCD mirror closed-loop data plots: (a) x-axis magnitude, (b) y-axis magnitude, (c) x-axis phase, and (d) y-axis phase.

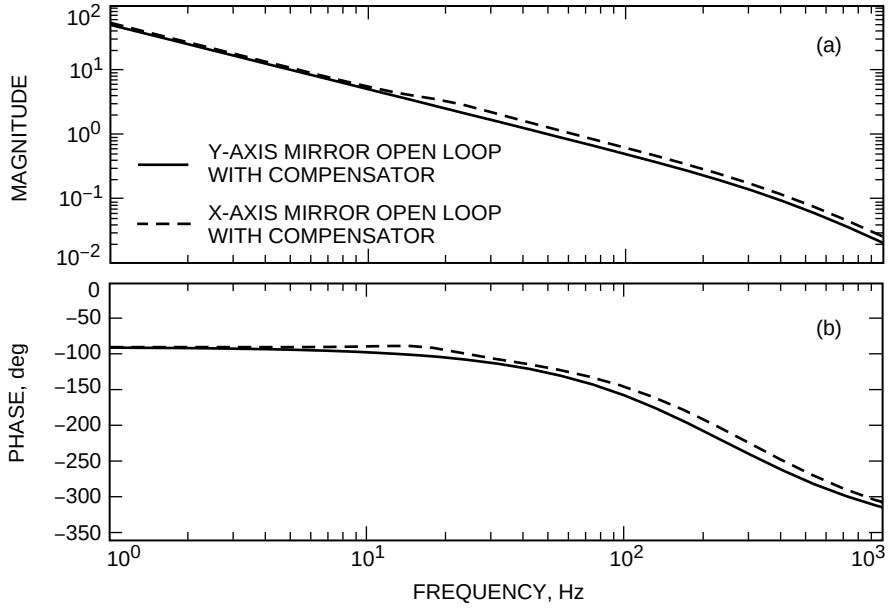

Fig. 7. The OCD mirror open-loop model with compensator: (a) magnitude and (b) phase.

slightly over 146 Hz, and the measured −3 dB bandwidth of the magnitude response was well over 100 Hz [Fig. 6(a)]. For the y-axis closed-loop control, the predicted −3 dB bandwidth of the magnitude response was near 177 Hz, but the actual −3 dB bandwidth turned out to be slightly over 110 Hz [Fig. 6(b)]. The predicted x-axis phase delay was −138 deg, and the measured phase delay was −126 deg, which is about 9 percent better than predicted [Fig. 6(c)]. The predicted y-axis phase delay at 100 Hz was about −110 deg [Fig. 6(d)], and the measured y-axis phase delay at 100 Hz was −126 deg, a 14.5 percent difference between the predicted and measured responses. These results are listed in Table 1. The discrepancy between the predicted and the measured curves at the higher frequencies, above 50 Hz by inspection, indicates that there are some non-negligible nonlinear effects in the real system.

Table 1. The OCD-mirror closed-position loop measured and predicted results.

Frequency-domain performance characteristics	X-axis		Y-axis	
	Measured	Predicted	Measured	Predicted
Magnitude, −3dB bandwidth	128.6 Hz	146 Hz	112.6 Hz	177 Hz
Phase, $f = 100$ Hz	−126 deg	−138 deg	−126 deg	−110 deg

The predicted and measured system-error responses, $R_x(s)$ and $R_y(s)$, for this closed-loop system also were examined. The transfer function of error over input for sine wave inputs at discrete frequencies was plotted along with the predicted error over input transfer function based on the MATLAB model (see Fig. 8). The analytical transfer functions used to derive the predicted $R(s) = E(s)]/[U(s)$ frequency-domain responses are

$$R_x(s) = \frac{E_x(s)}{U_x(s)} = \frac{1}{1 + C_x(s)M_x(s)H_x(s)} \tag{9}$$

$$R_y(s) = \frac{E_y(s)}{U_y(s)} = \frac{1}{1 + C_y(s)M_y(s)H_y(s)} \tag{10}$$

The terms $E_x(s)$ and $E_y(s)$ are the actuating signals. In the time domain, they represent the instantaneous tracking errors. Hence, the $R_x(s)$ and $R_y(s)$ transfer functions are a measure of how well the systems reject vibration over certain frequencies. In order to reduce the tracking error, the magnitudes of the error transfer functions in Eqs. (9) and (10) must be less than one over the operating frequency range [6]. The time-domain error response can be determined by taking the inverse Laplace transform of $E_x(s)$ or $E_y(s)$ for a given input, $U_x(s)$ or $U_y(s)$. In both axes, the 0-dB bandwidth of the vibration suppression is about 50 Hz.

VI. MATLAB-Model-Based Predictions

We want to predict system performance for a different mirror and different mirror drives. Assuming the new mirror can be well characterized by a second-order linear system, a MATLAB model was created for a mirror plant in which the first resonant frequency is $\omega_n = 50$ Hz with damping, $\xi = 0.5$. The proposed new mirror plant model, $M(s)$, is

$$M(s) = \frac{99,000}{s^2 + 100 \times 2\pi \times 0.5s + (50 \times 2\pi)^2} \tag{11}$$

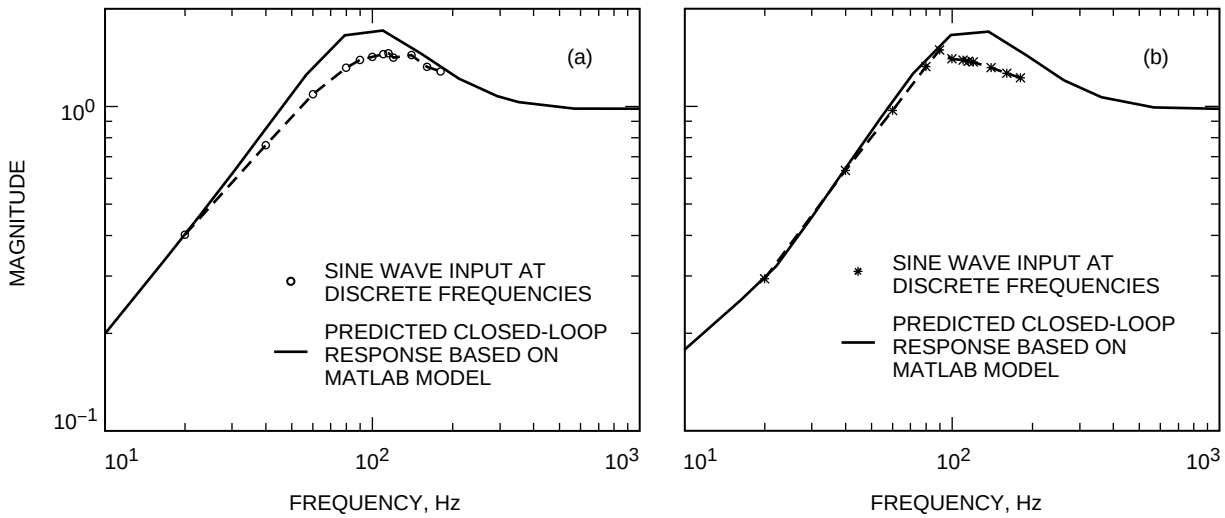

Fig. 8. The OCD mirror closed-loop (error/input) magnitude data plots: (a) x-axis and (b) y-axis.

Three separate cases are analyzed: the new mirror with no delay added, a second with a one-sample interval delay added, and a third with approximately a three-sample interval delay. Here, the sample interval is assumed to be 0.0005 second. The latter case is the delay that is present in the current system. The two cases with delay are modeled with the delay in the feedback path. Since this is a theoretical exercise, it is assumed that both axes of the new mirror are identical and not coupled. Hence, we will not be specific in terms of x- and y-axes. The digital filter, $C(z)$ in Eq. (12), was designed using stable plant pole cancellation as was done for the existing digital filter discussed in the previous sections:

$$C(z) = \frac{A[1 - 1.8318z^{-1} + 0.8546z^{-2}]}{1 - (1 + P_c)^{-1} + P_c z^{-2}} \tag{12}$$

where P_c is chosen to be a real valued number less than 1.0, and the choice for A, the forward gain, is a trade-off between system bandwidth and overshoot.

The digital filter equation was converted to its equivalent continuous time representation in the Laplace domain [see Eq. (13)]. The performance then was analyzed using continuous time domain techniques. For $P_c = 0.08$,

$$C(s) = \frac{A[s^2 + 3755.3s - 8,195,879.6]}{s^2 + 5051.4s - 1.6 \times 10^{-7}} \tag{13}$$

The delays were modeled by the transfer function H_i, where $i =$ the number of samples delay:

$$H_0(s) = 1 \tag{14}$$

$$H_1(s) = \frac{-s + 4000}{s + 4000} \tag{15}$$

$$H_3(s) = \frac{-s + 1200}{s + 1200} \tag{16}$$

The closed-loop transfer function then becomes

$$\frac{Y(s)}{U(s)} = \frac{A \times C(s)M(s)H_i(s)}{1 + A \times C(s)M(s)H_i(s)} \tag{17}$$

where $i = 0, 1,$ or 3.

For the case in which there is no delay in the system, $H_0(s)$, we choose $A = 80$ and $P_c = 0.08$ for the digital filter values. The closed-loop system response then indicates a 21.8 percent maximum overshoot and a −3dB bandwidth of approximately 900 Hz. If we add in a one-sample delay modeled by $H_1(s)$, then choose $A = 20$ and $P_c = 0.08$, the closed-loop response results in a maximum overshoot of 29 percent and a −3dB bandwidth of approximately 373 Hz. For the three-sample delay, $H_3(s)$, the choice of $A = 8$ and $P_c = 0.08$ results in a closed-loop response with a maximum overshoot of 32.8 percent and a −3dB bandwidth near 183 Hz. Table 2 summarizes these results. Figures 9(a) and (b) show the closed-loop magnitude and phase responses for all three cases. Notice that, to maintain a similar phase margin and maximum overshoot for all three cases, the forward gain and bandwidth are reduced significantly as the delay increases.

Table 2. The OCD-mirror closed-position loop predicted results.

Controller values			Results			
Time delay length	A	P_c	$f_{-3\text{dB}}$, Hz	Maximum overshoot, percent	Phase margin, deg	Gain margin, dB
No delay, H_0	80	0.08	903	21.8	48.76	12.2
1 sample delay, H_1	20	0.08	373	29	46.98	8.3
3 sample delay, H_3	8	0.08	178	32.8	47.09	7.6

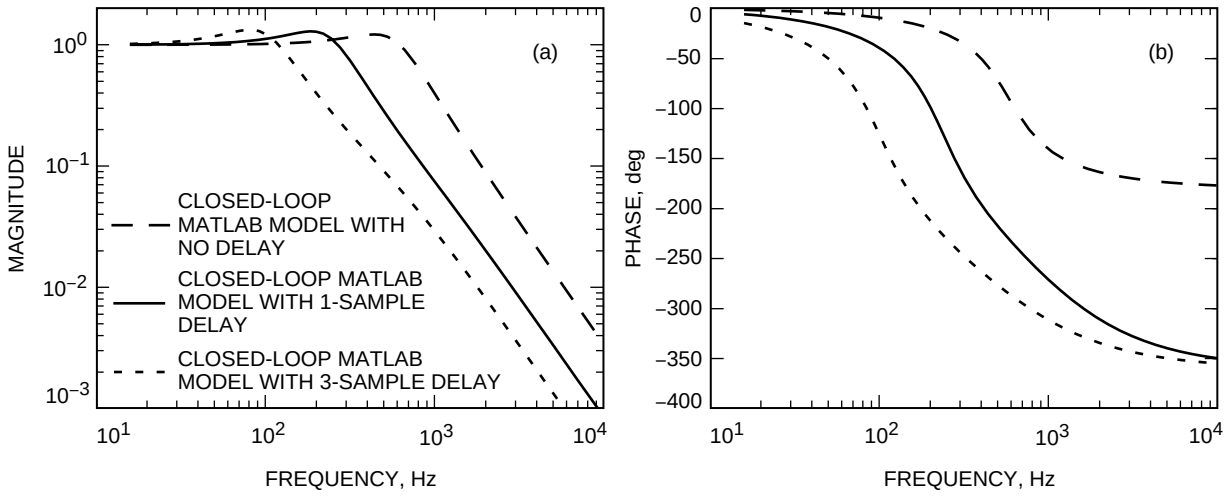

Fig. 9. The MATLAB model closed-loop predictions for a new mirror (with ω_n = 50 Hz): (a) magnitude and (b) phase.

In addition to the frequency-domain characteristics of the predicted system discussed above, the frequency-domain error-magnitude responses are plotted and shown in Fig. 10. These results demonstrate the effect of the tracking-loop delays on the system. For the case in which there is a three-sample delay added to the model of the new mirror, the error response is similar to the error response of the existing system. Since both axes of the mirror have similar error responses, only the y-axis of the existing mirror is included for reference. The modeling and simulations indicate that the system time delays must be minimized in order to improve the tracking performance, since any potential tracking performance improvements realized by upgrading to a better steering mirror may be diminished by the time delays contributed by the other components of the tracking loop.

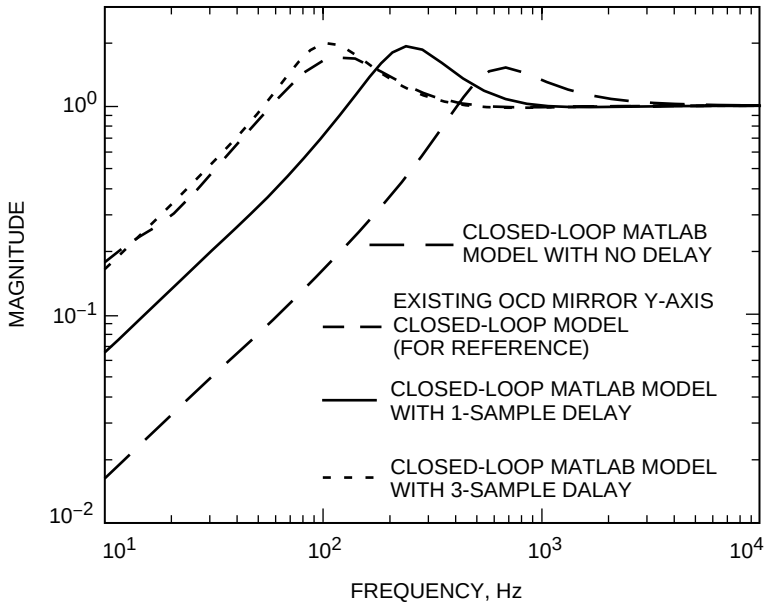

Fig. 10. The MATLAB model closed-loop (error/input) magnitude predictions for a new mirror (with ω_n = 50 Hz).

VII. Summary

This article characterizes the end-to-end digital-control system performance for the OCD. The frequency-domain characteristics of both the compensated and uncompensated systems were measured and modeled. Also, the time-domain response of the closed-loop system was simulated and compared with the measured response. A model-based analytical tool for performance prediction was developed for the OCD. This model then was used to predict performance for a new mirror. From the model and model-based simulations, we were able to deduce the effects of system delays on system performance. The real system also was modified to generate digital test inputs and allow for measurements to be gathered easily. Hence, the ability to collect real performance data is now part of the system. This feature provides for a systematic approach to quantifying any future upgrades to the OCD.

Acknowledgments

The authors would like to thank Tsun-Yee Yan for his technical support and encouragement and Kourosh Rahnamai for his helpful discussions.

References

[1] C. L. Phillips and H. T. Nagle, *Digital Control System Analysis and Design*, 2nd Edition, Englewood Cliffs, New Jersey: Prentice Hall, 1990.

[2] B. Shahian and M. Hassul, *Control System Design Using MATLAB*, Englewood Cliffs, New Jersey: Prentice Hall, 1993.

[3] T.-Y. Yan, M. Jeganathan, and J. R. Lesh, "Progress on the Development of the Optical Communications Demonstrator," *Free Space Laser Communication Technologies IX, SPIE Proceedings*, vol. 2990, San Jose, California, pp. 94–101, February 1997.

[4] H. Ansari, "Digital Control Design of a CCD-Based Tracking Loop For Precision Beam Pointing," *Free Space Laser Communication Technologies VI, SPIE Proceedings*, vol. 2123, Los Angeles, California, pp. 320–333, January 1994.

[5] J. S. Bendat and A. G. Piersol, *Random Data: Analysis and Measurement Procedures*, 2nd Edition, New York: John Wiley & Sons, 1986.

[6] R. C. Dorf, *Modern Control Systems*, 5th Edition, Menlo Park, California: Addison-Wesley Publishing Company, Inc., 1989.

[7] M. Jeganathan and S. Monacos, "Performance Analysis and Electronics Packaging of the Optical Communications Demonstrator," *Free Space Laser Communication Technologies X, SPIE Proceedings*, vol. 3266, San Jose, California, pp. 33–41, January 1998.

Appendix

Single Input–Single Output Model Estimates

The definitions and equations of the following data analysis procedure are from [5].

The time-series input data, $x(mt_s)$, and output data, $y(mt_s)$, with m a positive integer and t_s the sampling time, are detrended. Next, the data are passed through a Hanning filter to prevent spectral leakage in the Fourier domain.

The magnitude and phase responses of the system are estimated using the detrended filtered time-series data. The frequency-response estimate for a single-input/single-output system is calculated using the following:

$$\hat{H}_{xy}(f) = \frac{\hat{G}_{xy}(f)}{\hat{G}_{xx}(f)} = |\hat{H}_{xy}(f)|e^{-j\phi(f)} \tag{A-1}$$

where

$$\hat{G}_{xy}(f) = \frac{2}{N_d T} \sum_{i=1}^{N_d} X_i(f,T) \times Y_i^*(f,T) \tag{A-2}$$

is the averaged estimate of the one-sided cross-spectral density and

$$\hat{G}_{xx}(f) = \frac{2}{N_d T} \sum_{i=1}^{N_d} |X_i(f,T)|^2 \tag{A-3}$$

is the averaged estimate of the one-sided auto-sprectral density; $T = Nt_s$ is the length of the data subrecord in seconds; N is the number of data points in the data subrecord; $T_r = N_d T$ is the total record length of the data in seconds; N_d is the number of distinct and disjoint subrecords of length T seconds in the total record; t_s is the sampling time; $X_i(f,T)$ is the finite Fourier transform of the ith subrecord of the time series data, $x(mt_s)$; and $Y_i(f,T)$ is the finite Fourier transform of the ith subrecord of the time series data, $y(mt_s)$.

The system magnitude response is $|\hat{H}_{xy}(f)|$, and the system phase response is $\hat{\phi}(f)$. The estimated transfer function has values at discrete frequencies $f = f_k$, where $f_k = k/(Nt_s)$, for $k = 0, \cdots, N/2$.